

Insertable Stereoscopic 3D Surgical Imaging Device with Pan and Tilt

Tie Hu, Peter K. Allen, Tejas Nadkarni, Nancy J. Hogle and Dennis L. Fowler

Abstract—In this paper, we present an insertable stereoscopic 3D imaging system for minimally invasive surgery. It has been designed and developed toward the goal of single port surgery. The device is fully inserted into the body cavity and affixed to the abdominal wall. It contains pan and tilt axes to move the camera under simple and intuitive joystick control. A polarization-based stereoscopic display is used to view the images in 3D. The camera's mechanical design is based upon a single camera prototype we have previously built. We have run calibration tests on the camera and used it to track surgical tools in 3D in real-time. We have also used it in a number of live animal tests that included surgical procedures such as appendectomy, running the bowel, suturing, and nephrectomy. The experiments suggest that the device may be easier to use than a normal laparoscope since there is no special training needed for operators. The Pan/Tilt functions provide a large imaging volume that is not restricted by the fulcrum point of a standard laparoscope. Finally, the 3-D imaging system significantly improves the visualization and depth perception of the surgeon.

I. INTRODUCTION

Improving surgical imaging is a major goal, particularly in the field of Minimally Invasive Surgery (MIS), where surgeons are typically constrained by the use of a standard endoscope. Standard endoscopes suffer from the paradigm of pushing long sticks into small openings which is quite limiting. This approach has a number of problems including a narrow imaging field of view, limited work space, counter intuitive motions required by the operator, and multiple incisions for the endoscope ports and effector tooling. Despite these problems, this approach is still the state-of-the-art, even among advanced surgical robots such as the DaVinci system by Intuitive Surgical [7].

Our goal is to enhance and improve surgical procedures by placing small, mobile, multi-function platforms inside the body that can begin to assume some of the tasks associated with surgery [19], [16]. Our intent is to create a single port surgical system, where a single access port is used to introduce multiple sensors and effectors into the body cavity. Using new computer technology, we can remotize and control these devices inside the body using a variety of

visual and haptic interfaces. We want to create a feedback loop between new, insertable sensor technology and effectors we are developing, with both surgeons and computers in the information-processing/control loop.

Imaging technology for minimally invasive surgery has been significantly advanced in recent years[17], [5]. However, the 2D single lens endoscope is still the mainstream imaging device for MIS, with its attendant loss of depth perception. The basic architecture of the endoscope has not been fundamentally changed since the invention of the rod-lens by Hopkins and cold light source of fiber optics by Karl Storz in 1950's[4]. Traditional endoscopes use fiber-optics to deliver the light into the abdomen and the relayed lens and optical fibers to transmit the image back to the CCD camera sensor. The use of relayed lens and optical fibers significantly reduces the amount of light reaching the imaging sensors. Since the surgeon is generally working with both hands holding other instruments, an assistant is necessary to hold the endoscope steady and move it as required. Recent work in robotics has sought to automate that task. The Da Vinci surgical robot uses one robotic arm to hold the endoscope and control the motion[7]. While this takes the burden off the assistant and provides a much more stable image, it still occupies a large part of the operating room floor. A simpler robotic endoscope manipulator that can be placed directly over the insertion point was developed at INRIA[1], [15]. However, none of these systems addresses the fundamentally limited range of motion of the endoscope which is inherited from the Hopkins structure. The fulcrum point created by the abdominal wall restricts the motion of the scope to 4 degrees of freedom, so that the only translation possible is along the camera axis.

Other groups have been working on imaging devices for minimally invasive surgery or diagnosis with the goal of compact package and flexibility. One system uses a traditional rigid rod endoscope but adds a motor that rotates a 90-degree mirror at the end of the scope to provide an additional degree of freedom [6]. Another system is essentially a multi-link arm that positions a camera using piezoelectric actuators [12]. Theoretically this robot would provide many different viewing angles for an attached camera, but the authors provide no information about the safety of using piezoelectric electric elements, and do not appear to have attempted any tests within living animals or humans. The pill camera [22] is an example of a camera that operates entirely within the body. It is able to image sections of the small intestine that an endoscope cannot reach. However, it does not have any means of actuation and simply relies on peristalsis for locomotion.

This work was supported by NIH grant 1R21EB004999-01A1 and is subject to NIH Public Access Policy

Tie Hu is with Department of Computer Science, Columbia University, New York, NY10027 USA tie@cs.columbia.edu

Tejas Nadkarni is with Department of Computer Science, Columbia University, New York, NY10027 USA tgn2104@columbia.edu

Peter K. Allen is with Department of Computer Science, Columbia University New York, NY 10027 USA allen@cs.columbia.edu

Nancy J. Hogle is with Department of Surgery, Columbia University New York, NY 10032 USA nh2106@columbia.edu

Dennis L. Fowler is with Department of Surgery, Columbia University New York, NY 10032 USA dlf91@columbia.edu

The use of a stereoscopic set of cameras and a 3D display in minimally invasive surgery can compensate for the loss of 3D depth visualization [3]. Stereo imaging devices have many applications in medical robotics, such as augmented virtual reality surgery [5], tracking of the surgical tools and/or organs [21], 3D reconstruction of *in vivo* organ surfaces [2], [13], and NOTES surgery [14]. Stereo endoscopes have two basic optical structures: a dual lens system and a single lens system. In the dual lens system, the left and right lens capture slightly different images and transmit light to the individual image sensors through separate optical channels. The single lens system uses one lens to capture the image and split it into two images, which are captured by two image sensors. The single lens can achieve higher resolution and has more light than the dual lens system. However, both stereo endoscopes inherit the Hopkins rod-lens architecture.

II. MATERIALS AND METHODS

A. System Description

Our design goals in building this device were:

- Device must be fully insertable into body cavity, leaving the insertion port free for other sensors and tooling
- Device diameter must be restricted to 15 mm diameter for use with standard trocars.
- Pan and Tilt degrees of freedom required to increase internal imaging field of view
- 3D imaging required for proper depth perception
- Simple and intuitive control of the device
- Real-time response for Pan and Tilt to allow visual servoing and tracking
- User friendly 3D display system
- Low cost and possible disposal use

Figure 1 shows images of our implemented prototype device. The stereo device derives from the design of our previous single camera imaging devices described in [16], [9], [10], [11]. The total length of the device is 120mm, and the diameter is 15mm. After the surgeon inserts and anchors the device onto the abdomen wall inside the body, he can pan and tilt the camera to the desired surgical viewpoint using simple Joystick control. The device is designed to be easily disassembled and maintained, with a modular component design. Figure 2 shows a CAD model of the device. It has a stereo camera head module and a Pan/Tilt motion module. We use a 3D display from TrueVision, Inc. to display the images. It consists of a large screen on a mobile cart. Dual projectors rear-project the two stereo camera images on the screen, and the images are viewed using passive polarized glasses to restrict each image being viewed by only a single eye.

B. Design of Stereo Camera

Figure 3 shows the the CAD model of the stereo camera module. The enclosure is made from cylindrical plastic (Delrin). Two holes each with 6.5 mm in diameter were precisely aligned and drilled with the holes centered a distance of 7 mm apart. This is the inter-pupillary distance (IPD) we use for the stereo cameras. The external diameter of the enclosure



Fig. 1. Implemented Prototype Stereo Imaging Device with Pan/Tilt axes.

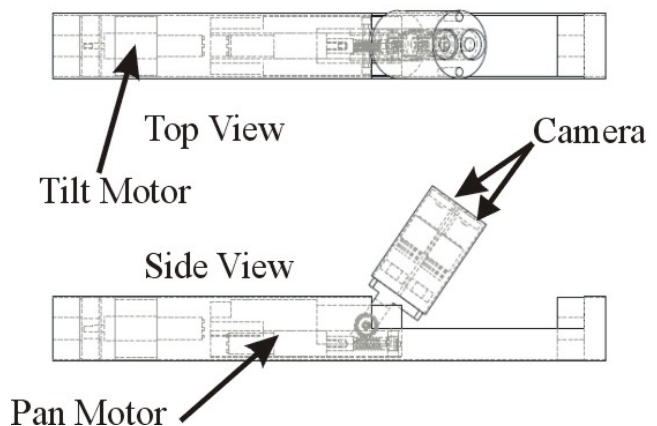
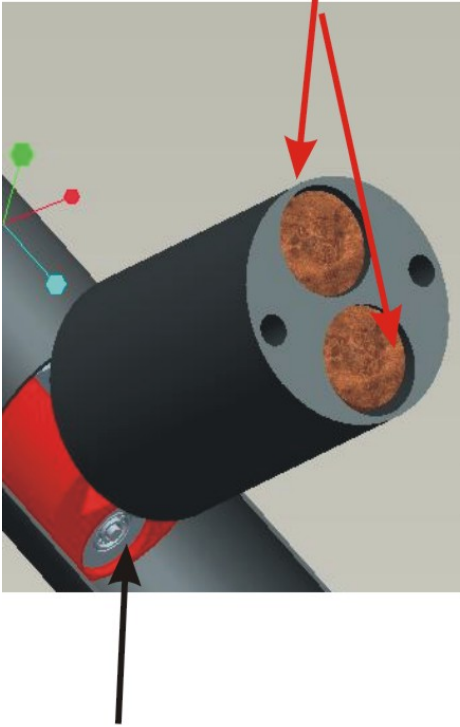


Fig. 2. CAD Model of Stereo Camera Device with Pan/Tilt.

Left and Right Camera



Pan Motor Bearing

Fig. 3. CAD Model of Stereo Camera Module

is 15 mm and the length is 25 mm. Each hole is used to host a micro camera.

We determined the optical characteristics of our lens using design criteria that included a 1) view distance (the distance between the lens and image object) as 40 mm to 100mm, 2) the view angle as 50 degrees, and 3) the active area on the CCD sensor as a circle 4.5mm in diameter. We used a miniature pin-hole lens (PTS 5.0 from Universe Kogaku America). The external casing of the lens was machined to 6.5mm. We use a $\frac{1}{4}$ " color video CCD camera head (Figure 4-Right) with outside diameter of 6.5 mm (NET USA Inc, CSH-1.4-V4-END-R1) in this package. The camera has active pixels of 752(H) X 582(V) at PAL system, which can provide 450 TV lines in horizontal resolution and 420 TV lines in vertical resolution. The lens was fixed to the front side of the hole by using glue. The CCD sensor was inserted into the hole and fixed by a set screw(0-80) after we precisely adjusted the focal plane (the view distance was set as 60 mm). Two semicircular parts tightly clamp the end of the CCD camera head wire. This design packages the fragile soldering point of the camera and insulates the terminator of the head from the stainless steel tube. Finally, a sapphire (Edmund Optics 9.5mm) is placed in front of lens and sealed with epoxy glue (Figure 4-Left).

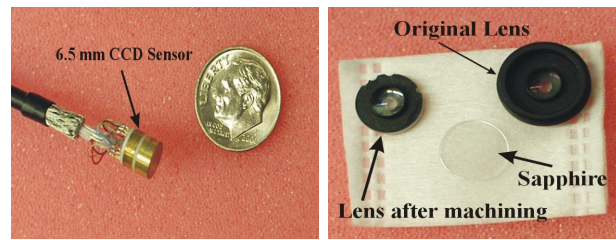


Fig. 4. Left: CCD Camera head. Right: Lens and Sapphire

C. Pan and Tilt Mechanism

The pan/tilt actuators are smoovy motors from Faulhaber-Group. They are fixed in the internal part of the device by set screws. A brushless DC motor (0513G, Smoovy, Inc) with 625:1 planetary gearhead(Series 06A , Smoovy, Inc) has a length of 27.0 mm and a diameter of 5.8 mm. It can deliver a torque of 25.0 mNm at continuous operation and 37.5 mNm at intermittent operation. For a motor with 125:1 planetary gearhead, it can generate 6.0 mNm at continuous operation and 9.0 mNm at intermittent operation. We used a worm gear mechanism to pan the camera module. It can transverse the motion in a compact size and increase the output torque. The worm gear (KLEISS Gear, Inc) has a gear reduction ratio of 16:1. A coupler was machined to connect the pan motor (125:1 gear ratio) axis and the worm (Figure 5 -Right). The other end of worm is supported by a sleeve sintered brass bearing so that the motor axis could be kept aligned with the worm axis. A gear transversely rotates through the movement of the worm. The camera module is linked with the axis of the gear by a joint. Two 3 mm ball bearings are used to reduce the rotational friction (Figure 1 -Right). Therefore, it can pan as the pan motor rotates. The axis of the tilt motor (625:1 gear ratio) is coaxially aligned with the external stainless steel tube and fixed with a coupler which is firmly attached to the external tube. A sleeve bearing made of sintered brass was machined to provide another support between the tilt part and external tube. The bearing can also reduce the friction force and smooth the tilt motion. Once the external tube is fixed on the wall of the abdomen, the camera module can tilt as the tilt motor rotates. The motor wires come out from the side of tilt motor coupler. The terminators of the motors were remade to fit into a 15 mm package. Figure 5-Left shows the modified motor terminal. Three magnetic wires were soldered into the three terminators of the motor and epoxy glued to seal the soldering point.

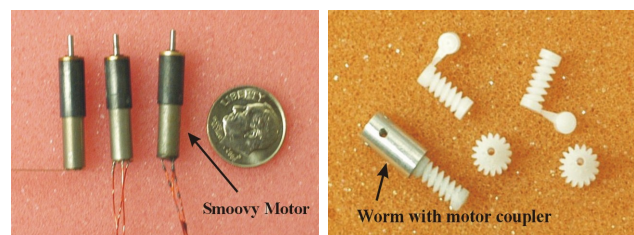


Fig. 5. Left: Smoovy motor with magnetic wire, Right: Worm gear.

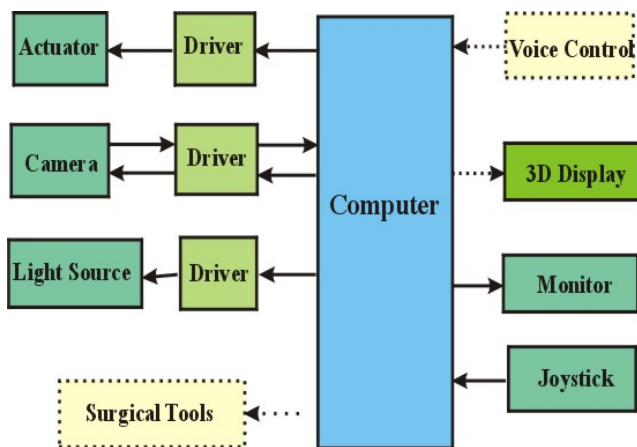


Fig. 6. System Configuration of new imaging device. Endoscope.

D. Design of the Control System

Figure 6 shows the configuration of the open-loop control system. The solid-line blocks show the current system's functions, which include Joystick control, video display, pan/tilt motion control, LED light source control, and stereo display. The dot-line blocks show the extendable functions in the future. The future system will include voice control, and surgical tooling attached to the platform. The computer is a standard PC (Intel Pentium III, 863 MHz, 384 MB RAM) with a Hauppauge frame grabber and a motion control board. Our single camera device has an integrated LED light source [9]. The control system can digitally control the light intensity of LED light source. The stereo camera device described in this paper does not yet have the LED lighting module, but it is under development.

The motion control board is a National Instruments NIDAQ PCI-6713 board with a SCB 68 break-out board, which can control the motor's direction, position and velocity. The NIDAQ board generates a series of control square waves to motor drivers (BLCPS.0002.8, Smoovy, Inc.), which directly output appropriate sequence current to the motor coils to drive the motor at certain speeds. By changing the frequency and pulses of control square wave, we can precisely control the velocity and position of motors. Software was developed to poll out the aileron and elevator position of the control Joystick, and use these parameters to control the pan and tilt motor's velocity, making for a very simple and efficient control interface.

The maximum motor speed is 15,000 rpm. For the tilt motor, a 625:1 gear ratio head was used to reduce the speed and increase the motor's torque. For the pan motor, a 125:1 gear ratio head was installed and connected with a 16:1 ratio's worm gear mechanism. Therefore, the speed range for tilt motor is from 0 to 24 rpm. The pan motion can achieve the maximum speed of 0.79 rad/sec.

III. EXPERIMENTAL RESULTS

A. Calibration of Stereo Cameras

We performed a standard DLT (Direct Linear Transform) calibration of each camera. In this procedure, 10 known 3-D

points on a calibration cube with a checkerboard pattern were imaged in each camera, and the calibration matrix was computed for each camera. Once these matrices were computed, the image points in each camera of the checkerboard corners were re-projected into the 3-D scene. The intersection point of these two camera rays from each camera was computed and compared against the known checkerboard corners 3-D coordinates. The average re-projection error for the 10 calibration points was 0.1578 mm. The calibration was over a working range of 70-90 mm in front of the cameras, distances that are typical for our surgical tasks.

B. Tracking Experiment

Once the cameras are calibrated, they can be used to track objects such as surgical tools in 3-D. We have built a color tracking system that can be used with a variety of surgical tools. The tracker works by tracking the centroid of an area in the image which is colored differently from the background. We initialize it by providing the coordinates of a pixel inside the area we are trying to track. Using the mean RGB values of region surrounding this pixel as a base, the tracker scans a neighborhood around the base coordinates for pixels whose RGB values are within an epsilon range from the base RGB values. By taking the mean of the coordinates of these pixels we get the centroid of the area to be tracked. In addition we found that taking the mean of the RGB values of these pixels to be the base RGB for the next iteration led to more reliable tracking as lighting changed over the images. By repeating this process for each frame we are able to track a colored area as it moves in the image. The length of the neighborhood to be scanned and the range of acceptable RGB values are parameters that can be changed depending on the object to be tracked. Figure 7 shows a tracking result for left camera as it follows an endoscopic grasping tool's trajectory.

As we track these designated regions in real-time in each calibrated camera, we can reproject the image points in both cameras to find the tracked region's 3D centroid coordinates using triangulation. Figure 8-top shows a plotted trajectory from a Flock of Birds real-time tracking system [8]. This system is accurate to .1 mm. We tracked this device using our cameras, and in Figure 8-bottom we have plotted the trajectory of the device computed in real-time by the stereo cameras.

C. Animal Experiments

We have used the imaging system in *in vivo* porcine animal tests. Laparoscopic surgeons performed a number of surgical procedures, including appendectomy, running (measuring) the bowel, suturing, and nephrectomy (kidney removal). Since this test animal species does not have an appendix as a human, resecting part of the colon was used to simulate an appendectomy.

In our animal experiments we compared the timings of each operation with using 1) a standard laparoscope imaging system and 2) our new 3D imaging system. One of the authors (Fowler) performed the surgical procedures and personnel without laparoscopic training operated each of

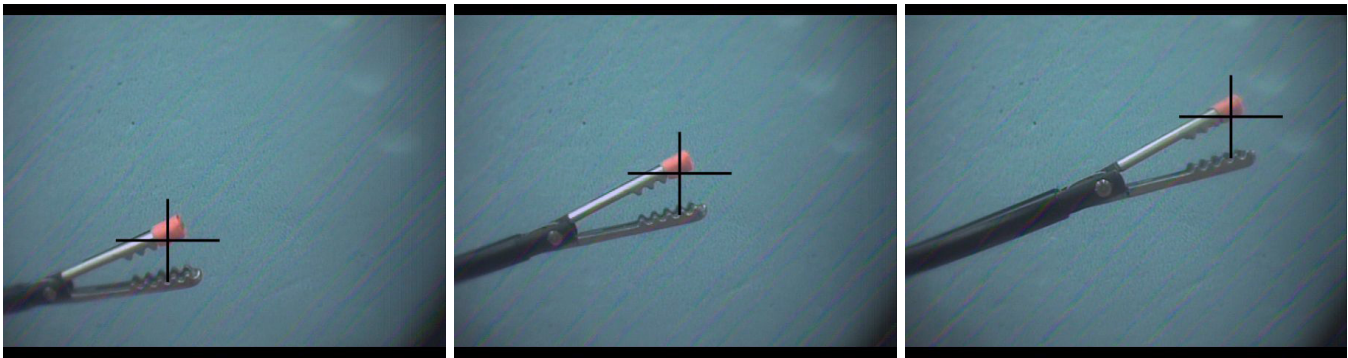


Fig. 7. Tracking a surgical instrument in left camera

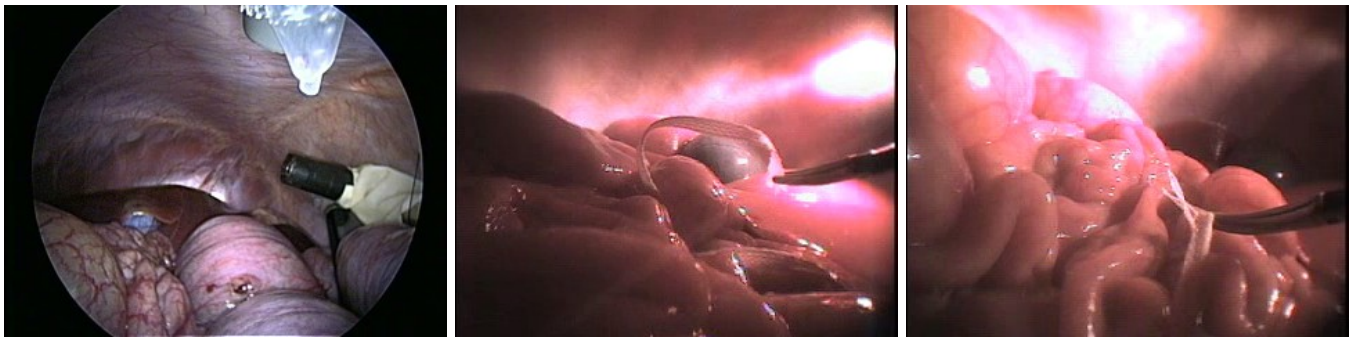


Fig. 9. In vivo animal experiment. Left: Device affixed to inside of abdominal wall as seen from a standard laparoscope. Center and Right: Images from left camera of stereo imaging device during running the bowel surgical task.

the devices. Figure 9 shows some images from one camera of the device, which was able to pan and tilt easily to accommodate the surgeon's need for new views of the surgical site. The surgical task shown is running the bowel. During this procedure, the surgeon used a flexible ruler to measure the length of bowel. As the surgeon moves the flexible ruler along the bowel, the cameras can pan and tilt to keep the ruler in the field of view.

While we cannot recreate the 3D imaging effect in a paper, we can report that it is quite powerful in providing a rich depth image that helps immensely in performing difficult surgical tasks such as suturing. One of the most difficult aspects of learning MIS is dealing with the lack of 3D depth perception. Our device provides full depth perception in a compact and simple system.

Figure 10 shows the timings of each procedure for both a standard laparoscope and our new device (only one nephrectomy was performed). The experiments suggest that this 3D imaging system significantly improves the visualization. In delicate suturing, the recovery of depth perception greatly helps the surgeon in speed and precision. The pan/tilt axes on the device can provide a large viewing volume without the restrictions caused by the fulcrum point of a standard laparoscope. It also suggests that the device may be easier to use than a normal laparoscope as there is no special training needed for the operator of the imaging device.

IV. CONCLUSIONS AND FUTURE WORK

This paper describes a 3D imaging system for laparoscopic surgery. The intent is to create totally insertable surgical imaging systems which do not require a dedicated surgical port, and allow more flexibility and DOF's for viewing. We have used the device for 3D tracking of surgical tools and in live animal experiments we have performed laparoscopic appendectomy, running the bowel, suturing, and nephrectomy.

Issues that still need to be addressed include sealing and sterilization of the unit and mounting the device on the abdominal wall. Our camera module is a sealed unit, so it may be possible to sterilize it chemically. The device is currently mounted by suturing the device to the inside of the abdominal wall. We tested this using a standard laparoscope to assist in the mounting. In the future, we hope to be able to develop a spring mounted system that will allow the device to be sutured without using a standard laparoscope. Magnetic attachment is also a possibility [20].

We believe these insertable platforms will be an integral part of future surgical systems. The platforms can be used with tooling as well as imaging systems, allowing some surgical procedures to be done using such a platform. The system can be extended to a multi-functional surgical robot with detachable end-effectors (grasper, cutting, dissection and scissor). Because the systems are insertable, a single surgical port can be used to introduce multiple imaging and tooling platforms into a patient.

One of our design goals is to simplify the control of

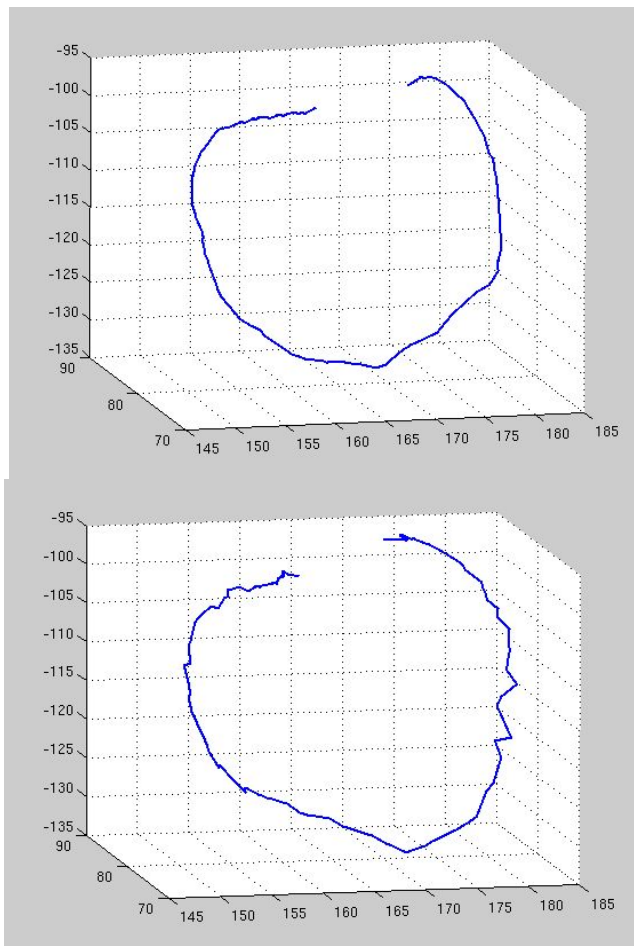


Fig. 8. Top: 3-D Plotted trajectory of Flock of Birds sensor. Bottom: 3-D Plotted trajectory of Flock of Birds sensor using stereo re-projection from our imaging device in real-time.

Procedure	Device	Time (min)
Running Bowel	Laparoscope	5:35
Running Bowel	Robot	3:14
Appendectomy	Laparoscope	1:57
Appendectomy	Robot	1:38
Suturing	Laparoscope	4:30
Suturing	Robot	2:12
Nephrectomy	Robot	9:59

Fig. 10. Procedure Timings

the imaging system. One possible approach to controlling the cameras would be to use a hybrid controller, which allows the surgeon to control some of the degrees-of-freedom (DOF) of the device and an autonomous system, which controls the remaining DOF. For example, the autonomous system can control pan/tilt on the camera to keep a surgeon-identified organ in view, while the surgeon simultaneously may translate the camera to obtain a better viewing angle - all the while keeping the organ centered in the viewing field. We have developed hybrid controllers similar to this for robotic work-cell inspection [18] and believe we can transfer these methods for use with this device.

REFERENCES

- [1] P. Berkelman, P. Cinquin, J. Troccaz, J. Ayoubi, C. Letoublon, and F. Bouchard. A compact, compliant laparoscopic endoscope manipulator. In *IEEE Intl. Conf. on Robotics and Automation*, pages 1870–1875, 2002.
- [2] D. Stoyanov, A. Darzi, and G.Z. Yang. A practical approach towards accurate dense 3d depth recovery for robotic laparoscopic surgery. *Computer Aided Surgery*, 10(4):199–208, July 2005.
- [3] A. F. Durrani and G. M. Preminger. Three-dimensional video imaging for endoscopic surgery. *Comput. Biol. Med.*, 25:237–247, 1995.
- [4] G. J. Fuchs. Milestones in endoscope design for minimally invasive urologic surgery: the sentinel role of a pioneer. *Surg Endosc.*, 20:493–499, 2006.
- [5] H. Fuchs, M. A. Livingston, R. Raskar, D. Colucci, K. Keller, A. State, J. R. Crawford, P. Rademacher, S. H. Drake, and A. A. Meyer. Augmented reality visualization for laparoscopic surgery. In *Medical Image Computing and Computer-Assisted Intervention-MICCAI*, 1998.
- [6] L. M. Gao, Y. Chen, L. M. Lin, and G. Z. Yan. Micro motor based new type of endoscope. In *Intl. Conf of the IEEE Engineering in Medicine and Biology Society*, volume 20, pages 1822–1825, 1998.
- [7] G. Guthart and K. Salisbury. The Intuitive telesurgery system: Overview and application. In *IEEE International Conference on Robotics and Automation*, pages 618–621, 2000.
- [8] <http://www.ascensiontech.com/products/flockofbirds.php>.
- [9] T. Hu, P. K. Allen, and D. L. Fowler. In vivo pan/tilt endoscope with integrated light source. In *IEEE/RSJ International Conference on Intelligent Robots and Systems (IROS)*, Oct 29–Nov 2 2007.
- [10] T. Hu, P. K. Allen, R. Goldman, N. J. Hogle, and D. L. Fowler. In vivo pan/tilt endoscope with integrated light source, zoom and auto-focusing. In *Medicine Meets Virtual Reality (MMVR) 16*, January 30–February 1 2008.
- [11] T. Hu, P. K. Allen, N. J. Hogle, and D. L. Fowler. Insertable surgical imaging device with pan, tilt, zoom and lighting. In *International Conference on Robotics and Automation (ICRA)*, May 19–23 2008.
- [12] K. Ikuta, M. Nokata, and S. Aritomi. Biomedical micro robots driven by miniature cybernetic actuator. In *IEEE Workshop on Micro Electromechanical Systems*, pages 263–268, 1994.
- [13] W. W. Lau, N. A. Ramey, J. J. Corso, N. V. Thakor, and G. D. Hager. Stereo-based endoscopic tracking of cardiac surface deformation. In *Medical Image Computing and Computer-Assisted Intervention-MICCAI*, pages 494–501, 2004.
- [14] A. C. Lehman, J. Dumpert, N. A. Wood, A. Q. Visty, S. M. Farritor, and D. Oleynikov. In vivo robotics for natural orifice transgastric peritoneoscopy. In *Medicine meets Virtual Reality 16*, volume 132, pages 236–241, 2008.
- [15] J. Ma and P. Berkelman. Task evaluation of a compact laparoscopic surgical robot system. In *Proceedings of the 2007 IEEE/RSJ International Conference on Intelligent Robots and Systems*, pages 398–403, Oct 29–Nov 2 2007.
- [16] A. Miller, P. Allen, and D. Fowler. In-vivo stereoscopic imaging system with 5 degrees-of-freedom for minimal access surgery. In *Medicine Meets Virtual Reality (MMVR)*, 2004.
- [17] R. Mochizuki and S. Kobayashi. HDTV single camera 3d system and its application in microsurgery. In *SPIE Vol. 2177*, 1994.
- [18] P. Oh and P. Allen. Visual servoing by partitioning degrees-of-freedom. *IEEE Trans. on Robotics and Automation*, 17:1–17, February 2001.
- [19] D. Oleynikov, M. Rentschler, M. Hadzialic, A. Dumpert, J. Platt, and S. Farritor. Miniature robots can assist in laparoscopic cholecystectomy. *Journal of Surgical Endoscopy*, 19(4):473–476, 2005.
- [20] S. Park, R. Bergs, R. Eberhart, L. Baker, R. Fernandez, and J. A. Cadeddu. Trocar-less instrumentation for laparoscopy magnetic positioning of intra-abdominal camera and retractor. *Annals of Surgery*, 245(3):379–384, 2007.
- [21] G.Q. Wei, K. Arbter, and G. Hirzinger. Real-time visual servoing for laparoscopic surgery. *IEEE Engineering in Medicine and Biology*, pages 40–45, January 1997.
- [22] M. Yu. M2a capsule endoscopy: A breakthrough diagnostic tool for small intestine imaging. *Gastroenterology Nursing*, 25:24–27, 2002.